J. Cell. Mol. Med. Vol 22, No 3, 2018 pp. 1944-1956

# Increased free $Zn^{2+}$ correlates induction of sarco(endo)plasmic reticulum stress *via* altered expression levels of $Zn^{2+}$-transporters in heart failure

**Yusuf Olgar [a, #], Aysegul Durak [a, #], Erkan Tuncay [a], Ceylan Verda Bitirim [a], Evren Ozcinar [b], Mustafa Bahadir Inan [b], Zeynep Tokcaer-Keskin [c], Kamil Can Akcali [a], Ahmet Ruchan Akar [b], Belma Turan [a, *]**

[a] *Department of Biophysics, Ankara University Faculty of Medicine, Ankara, Turkey*
[b] *Department of Cardiovascular Surgery, Heart Center, Ankara University Faculty of Medicine, Ankara, Turkey*
[c] *Department of Molecular Biology, Acibadem University, Istanbul, Turkey*

*Received: July 1, 2017; Accepted: October 29, 2017*

## Abstract

$Zn^{2+}$-homoeostasis including free $Zn^{2+}$ ($[Zn^{2+}]_i$) is regulated through $Zn^{2+}$-transporters and their comprehensive understanding may be important due to their contributions to cardiac dysfunction. Herein, we aimed to examine a possible role of $Zn^{2+}$-transporters in the development of heart failure (HF) *via* induction of ER stress. We first showed localizations of ZIP8, ZIP14 and ZnT8 to both sarcolemma and S(E)R in ventricular cardiomyocytes (H9c2 cells) using confocal together with calculated Pearson's coefficients. The expressions of ZIP14 and ZnT8 were significantly increased with decreased ZIP8 level in HF. Moreover, $[Zn^{2+}]_i$ was significantly high in doxorubicin-treated H9c2 cells compared to their controls. We found elevated levels of ER stress markers, GRP78 and CHOP/Gadd153, confirming the existence of ER stress. Furthermore, we measured markedly increased total PKC and PKCα expression and PKCα-phosphorylation in HF. A PKC inhibition induced significant decrease in expressions of these ER stress markers compared to controls. Interestingly, direct increase in $[Zn^{2+}]_i$ using zinc-ionophore induced significant increase in these markers. On the other hand, when we induced ER stress directly with tunicamycin, we could not observe any effect on expression levels of these $Zn^{2+}$ transporters. Additionally, increased $[Zn^{2+}]_i$ could induce marked activation of PKCα. Moreover, we observed marked decrease in $[Zn^{2+}]_i$ under PKC inhibition in H9c2 cells. Overall, our present data suggest possible role of $Zn^{2+}$ transporters on an intersection pathway with increased $[Zn^{2+}]_i$ and PKCα activation and induction of HF, most probably *via* development of ER stress. Therefore, our present data provide novel information how a well-controlled $[Zn^{2+}]_i$ *via* $Zn^{2+}$ transporters and PKCα can be important therapeutic approach in prevention/treatment of HF.

**Keywords:** zinc transporters • intracellular zinc • heart failure • endoplasmic reticulum stress • left ventricle

## Introduction

Advanced HF is an irreversible process while numerous different signalling pathways and mechanisms are involved during its development. The association between defective cardiac activity and altered cellular $Ca^{2+}$-homoeostasis is well characterized in HF [1]. Emerging evidence suggests a central role of intracellular-free $Zn^{2+}$ ($[Zn^{2+}]_i$) in excitation–contraction coupling in cardiomyocytes by shaping $Ca^{2+}$ dynamics [2, 3]. Experimental and clinical studies have also shown that several proteins, having pivotal role in controlling cardiac contractility, are also potential targets of $[Zn^{2+}]_i$ as well as $[Ca^{2+}]_i$ [4, 5]. Zinc as $Zn^{2+}$ is required for structure and function of cells and its availability, *via* interprotein $Zn^{2+}$-binding sites, influences functions of numerous proteins in mammalian cells [6]. Therefore, any impairment in $[Zn^{2+}]_i$ homoeostasis may result in a variety of cellular dysfunction including cardiomyocytes, which may in turn induce serious cardiovascular pathologies [7].

Cellular $[Zn^{2+}]_i$ is tightly regulated against its adverse effects through either $Zn^{2+}$ transporters, $Zn^{2+}$-binding molecules or $Zn^{2+}$ sensors, and, therefore plays a critical role in cellular signalling pathways [8, 9]. In addition, it has been suggested that $[Zn^{2+}]_i$ associated with cellular signalling mechanisms can be classified

[#]Equally contributed to the study as first authors.
*Correspondence to: Belma Turan, PhD
E-mail: belma.turan@medicine.ankara.edu.tr

doi: 10.1111/jcmm.13480

by time windows, such as early $Zn^{2+}$ signalling within several minutes as well as late $Zn^{2+}$ signalling within several hours following its intracellular increase [7]. However, it remains unclear whether these suggested signalling effects are independent, combinatory or cell-dependent. Most of $[Zn^{2+}]_i$-associated cellular events arised due to either the effect of mobile reactive/free $Zn^{2+}$ but not on the non-exchangeable $Zn^{2+}$. Free $Zn^{2+}$ participates in redox homoeostasis on sarco(endo)plasmic reticulum {S(E)R} function and mitochondrial metabolism, as well [10–14]. Only few studies have documented the role of $Zn^{2+}$ homoeostasis in cardiovascular dysfunction. These studies reported the role of $Zn^{2+}$ dyshomeostasis in the pathogenesis of myocardial ischaemia/reperfusion injury [15], the role of a $Zn^{2+}$ transporter, ZIP12, in the regulation of the pulmonary vascular response to chronic hypoxia [16] and the role of crosstalk between ZnT-1 and the L-type $Ca^{2+}$ channels in cardiac electrical remodelling of adult rat atrium and in humans with atrial fibrillation [17, 18].

ER stress is one of the underlying mechanisms of major diseases associated with cardiac dysfunction including diabetic cardiomyopathy [10, 19]. Indeed, we have previously shown that S(E)R function can be normalized when $[Zn^{2+}]_i$ is kept at normal level *via* enhancement of the antioxidant defence in diabetic rats [3, 11]. Recently, we have shown that $Zn^{2+}$ decrease in S(E)R leads to the up-regulation of ER stress confirming the requirement of $Zn^{2+}$ for proper S(E)R function [20]. However, there are no clear data on the role of $Zn^{2+}$ transporters controlling $[Zn^{2+}]_i$ in cardiomyocytes during the progression of HF, and, further studies are needed to clarify this important possible relation.

Excess $[Zn^{2+}]_i$ could affect the function of the ZIP and ZnT families, including the enhancements of protein kinase C (PKC) signalling and activation in Akt and ERK pathways [21]. Particularly, free $[Zn^{2+}]_i$ can increase the activity of PKC by contributing to its binding to plasma membrane and hence play a crucial role in many signal transduction pathways [21–23]. Furthermore, one isoform of PKC, PKC$\alpha$, has been shown to have unique properties among other PKC isotypes in terms of induction of cardiac hypertrophy, and regulation of contractility and HF susceptibility [24–26]. Moreover, we recently have shown that hyperglycaemia induced marked changes in ZIP7 and ZnT7 expression levels underlined excess $Zn^{2+}$ release from S(E)R and could mediate ER stress in the heart [20].

Therefore, in this study, we first aimed to test the possible roles of some $Zn^{2+}$ transporters in the development of HF *via* induction of ER stress. For this purpose, we, for the first time, monitored subcellular localizations of $Zn^{2+}$ transporters such as ZIP8, ZIP14 and ZnT8 in cardiomyocytes. We also examined the role of $[Zn^{2+}]_i$ in HF-modelled cardiomyocytes with doxorubicin-treated cells (embryonic left ventricular rat heart cell line, H9c2 cells) and protein expressions levels of these $Zn^{2+}$ transporters in human HF samples (end-stage failing hearts, due to dilated or ischaemic cardiomyopathy) and in HF-modelled cells. Lastly, we monitored the onset of ER stress using its markers such as GRP78, CHOP/Gadd153 and calnexin as well as phosphorylation level of PKC$\alpha$ in heart preparations or in directly $[Zn^{2+}]_i$ increased cardiomyocytes.

# Materials and methods

## Patients and tissues

Patients, who were scheduled to undergo orthotopic heart transplantation for end-stage HF at the Department of Cardiovascular Surgery of Ankara University Faculty of Medicine, were eligible to participate in the study. The Local Ethics Committee of Ankara University approved the study protocol (1003201404-142-14). The investigation conforms to the principles outlined in the Declaration of Helsinki. All participating patients signed informed written consent before surgery. Left ventricular tissues were collected from discarded hearts of advanced HF patients. The cause of HF was dilated cardiomyopathy (DCMP) in two patients, and one patient had ischaemic cardiomyopathy (ICMP). Control left ventricular tissues were obtained from deceased donors that were unsuitable for cardiac transplantation. Donor families were also consented to use of the cardiac tissues for research. Clinical characteristics of patients and controls are given in Table 1.

## Cell line and treatment of cells with doxorubicin

We used cardiac myoblasts from left ventricle of the embryonic rat heart (ATCC CRL1446; purchased from American Type Culture Collection, Manassas, VA). Cells were grown at a density of about $10^5$ cells/$cm^2$ in DMEM modified using 5.5 mM glucose instead of 25 mM and supplemented with 10% foetal calf serum, 50 U/ml penicillin-G and 50 $\mu$g/ml streptomycin in a humidified atmosphere of 95% air and 5% $CO_2$ at 37°C.

To model HF in cardiomyocytes, the procedure as described previously was performed [27]. The cultured H9c2 cardiomyocytes in media containing 0.5% bovine serum albumin were treated with a doxorubicin analog agent adriamycin (1 $\mu$M for 24 hrs) at 37°C. Cell viability and apoptosis were evaluated by MTT cell viability assay and some apoptosis-related signal proteins.

## Localization examination of $Zn^{2+}$ transporters

Localizations of $Zn^{2+}$ transporters, ZIP8, ZIP14 and ZnT8 in cardiomyocytes were determined using anti-ZIP8 (ProteinTech, Rosemont, IL, USA, 20459-1; 1:50), anti-ZIP14 (ThermoFisher, Waltham, MA, USA, PA5-21077; 1:50) and anti-ZnT8 (SantaCruz, Dallas, Texas, USA, sc98243; 1:50) antibodies, using confocal microscopy (Zeiss LSM 700). The S(E)R localization was determined by transfection of H9c2 cells with plasmids encoding ER-resident Discosoma red fluorescent protein (dsRED-ER(red) as a manner of 2 $\mu$g per well in a 6-well plate) using Lipofectamine 2000 for 24 hr. After fixation and permeabilization of H9c2 cells with 4% paraformaldehyde and 0.3% Triton-X100, respectively, they were incubated with ZIP8, ZIP14 and ZnT8 antibody to monitor the localization of ZIP8, ZIP14 and ZnT8 protein in the S(E)R. After overnight incubation of the cells, they were further incubated with appropriate secondary antibodies in the presence of 5% (w/v) BSA (Alexa Fluor 488 Donkey anti-Rabbit for ZIP8 and ZnT8 (green); 1:1000, Alexa Fluor 488 Rabbit anti-Goat for ZIP14 (green); 1:1000).

Plasma membrane was labelled using a plasma membrane marker anti-plasma membrane $Ca^{2+}$-ATPase (PMCA) monoclonal antibody (ThermoFisher; MA3-914; 1:100). After fixation and permeabilization,



Journal of Cellular and Molecular Medicine published by John Wiley & Sons Ltd and Foundation for Cellular and Molecular Medicine.

**Table 1** Characteristics and haemodynamic performance of patients and controls

| Gender | Age (years) | LVEF (%) | PCWP (mmHg) | PVR (Wood) | CI (l/min/m$^2$) | PA (mmHg) | Diagnosis |
|---|---|---|---|---|---|---|---|
| Male | 46 | 65 | 11 | 1.6 | 3.8 | 25 | DD |
| Male | 57 | 60 | 13 | 2.6 | 2.9 | 35 | DD |
| Male | 31 | 10 | 33 | 3.6 | 1.52 | 62 | DCMP |
| Male | 46 | 15 | 11 | 2.0 | 2.5 | 24 | ICMP |
| Male | 48 | 15 | 18 | 2.9 | 1.27 | 35 | DCMP |

LVEF, left ventricular ejection fraction; PCWP, pulmonary capillary wedge pressure; PVR, pulmonary vascular resistance; CI, cardiac index; PA, pulmonary arterial pressure; DD, deceased donor; DCMP, dilated cardiomyopathy; ICMP, ischaemic cardiomyopathy.

H9c2 cells were incubated plasma membrane marker PMCA and ZIP8, ZIP14 or ZnT8 antibody separately to demonstrate the localization of the transporters on plasma membrane. Following overnight incubation, cells were further incubated with appropriate secondary antibodies (Alexa Fluor 488 Donkey anti-Rabbit for ZIP8 and ZnT8 (green); 1:1000, Alexa Fluor 488 Rabbit anti-Goat for ZIP14 (green); 1:1000 and Alexa Fluor 555 Goat anti-Mouse for PMCA (red); 1:1000) and were mounted with medium containing DAPI (blue). Images for co-localization were analysed and processed using JACOP imageJ plugin.

## Intracellular-free $Zn^{2+}$ measurement in H9c2 cells

To monitor the basal (resting) level of intracellular-free $Zn^{2+}$ ($[Zn^{2+}]_i$) in H9c2 cells, we used a $Zn^{2+}$ sensitive fluorescence dye-loaded cells, using non-ratiometric FluoZin-3 (3-μM FluoZin-3 AM) for confocal microscope (LEICA SP5). Florescence intensities were acquired at 1 Hz, 490 nm excitation wavelength and collected at 525 nm. Image analysis was performed with ImageJ software. The steady state fluorescence intensity ($F$) was measured, then maximum and minimum ratios were determined to calculate free $Zn^{2+}$ level using the following formula: $[Zn^{2+}] = K_d(F-F_{min})/(F_{max}-F)$, where the $K_d$ for FluoZin-3 is 15 nM. The maximum fluorescence ($F_{max}$) was obtained upon $Zn^{2+}$ saturation with $Zn^{2+}$ salt of 1-hydroxypyridine-2-thione, $Zn^{2+}$-pyrithione ($Zn^{2+}$/Pyr; 10 μM), and the minimum ratio ($R_{min}$) was obtained upon intracellular $Zn^{2+}$ chelation with N, N, N', N'-tetrakis(2-pyridylmethyl)ethylenediamine (TPEN; 50 μM).

## Western blot analysis

Following pulverization of the samples at liquid nitrogen and homogenization, the lysates and tissues homogenates were extracted with NP-40 lysis buffer (250 mM NaCl, 1% NP-40 and 50 mM Tris-HCl; pH 8.0 and 1XPIC). The protein concentrations of supernatants after centrifugation (12,000 × g, 5 min. at 4°C) were measured with the BCA assay kit (Thermo Scientific Pierce, Waltham, MA USA) according to manufacturer's instructions. Equal protein amounts were separated on 12% SDS-PAGE Tris-glycine or 4–12% Bis-Tris gels (Thermo Scientific, Life Technologies, Waltham, MA, USA), as appropriate. Proteins were transferred to PVDF membranes and blocked with 4% BSA in PBS-Tween. Membranes were probed overnight with primary antibodies diluted in 4% BSA in PBS-Tween. The membranes were probed with antibodies against ZIP8 (Protein Tech, 20459-1-AP; 1:300), ZnT8 (Santa Cruz, Sc98243; 1:100), ZIP14 (Thermo, PA5-21077; 1:300), GRP78 (Santa Cruz, Sc13968; 1:200), CHOP/Gadd153 (Santa Cruz, Sc7351, 1:500), Calnexin (Santa Cruz, Sc11397; 1:300), total PKC (Santa Cruz, Sc80; 1:250), PKCα (Santa Cruz, Sc208; 1:100), phospho-PKCα (Santa Cruz, Sc12356; 1:100), CK2 (α1/2; Santa Cruz, Sc12738; 1:300), PUMA (α/β, Santa Cruz, Sc28226; 1:250), α-actinin (PA517308, Thermo Fisher Sci.), PKC inhibitor (GF109203X hydrochloride, Sigma-Aldrich), GAPDH (Santa Cruz, Sc365062; 1:1000) and β-actin (Santa Cruz, Sc47778; 1:500) in BSA/PBS/Tween-20 solution. Specific bands were visualized with HRP-conjugated compatible secondary antibodies (anti-mouse: 1:7500, anti-goat: 1:7500, anti-rabbit: 1:2000) and detected by ImmunoCruz Western Blotting Luminol Reagent (Santa Cruz, Sc2048). The density of bands was analysed using ImageJ software.

## Statistical analysis

Continuous data were expressed as mean (±S.E.M.), and categorical data as percentages. Groups were tested and compared using one-way ANOVA and Tukey post hoc test. A value of $P \leq 0.05$ was considered statistically significant. For all data, no statistics were used for predetermination of the sample size, randomization or blinding.

# Results

## Outcome of patients

We used left ventricular samples from three patients and two controls. Three patients underwent orthotopic heart transplantation with end-stage HF. One of these patients had ICMP while the other two had DCMP (HF group). We obtained control group samples from deceased donors that were unsuitable for cardiac transplantation (DD group). Both controls have good left ventricular function. One control deceased donor had Hepatitis C, and the other heart of the deceased donor was discarded because of persistant hypovolemic shock due to multiple traumatic injuries. The haemodynamic characteristics of patients and controls are summarized in Table 1. As mentioned previously, an important biochemical marker in heart failure is B-type

natriuretic peptide (BNP), which is produced in heart ventricles in response to increased mechanical load and wall stretch [28]. Therefore, before undergoing orthotopic heart transplantation with end-stage HF, the plasma BNP levels were measured in patients. The BNP level was in the range of 3000–4000 pg/ml in group of HF while this value was 2000–2400 pg/ml in DD group. The difference between these two groups is significantly different from each other ($P < 0.001$).

## Demonstration of subcellular localizations of ZIP8, ZIP14 and ZnT8 in cardiomyocytes

To test whether ZIP8, ZIP14 and ZnT8 are localized to either on S(E)R, sarcolemma or both, the cells were co-incubated with plasma membrane marker antibody (PMCA) and ZIP8, ZIP14 or ZnT8 primary antibodies after fixation and permeabilization. Images were captured using confocal microscopy and then merged (Fig. 1A–F). The Pearson's coefficients (PC) were calculated using Huygens programme for co-localization values of on either S(E)R or sarcolemma ZIP8 (A and B), ZIP14 (C and D) and ZnT8 (E and F). The calculated PCs from images for ZIP8-S(E)R and ZIP8-PMCA are $0.44 \pm 0.03$ and $0.60 \pm 0.02$, while these values for ZIP14 and ZnT8 are $0.50 \pm 0.08$ *versus* $0.66 \pm 0.03$ and $0.42 \pm 0.05$ *versus* $0.80 \pm 0.02$.

Our PCs' values strongly support the localization of these three $Zn^{2+}$ transporters on sarcolemma as about over 60% in mammalian ventricular cardiomyocytes. Additionally, our data demonstrated that these transporters were also localized on the S(E)R of the cardiomyocytes as about 40–50% due to calculated PCs' values.

## Altered expression levels of the $Zn^{2+}$ transporters in heart failure

We examined first the expression levels of $Zn^{2+}$ transporters ZIP8, ZIP14 and ZnT8 in human heart tissue. Western blot analysis showed that the expression levels of ZIP14 and ZnT8 were significantly higher than those of controls, whereas ZIP8 level was significantly lower comparison to the control (Fig. 2A, right) while the representative Western blot images are given also in the same figure, as well (Fig. 2A, left).

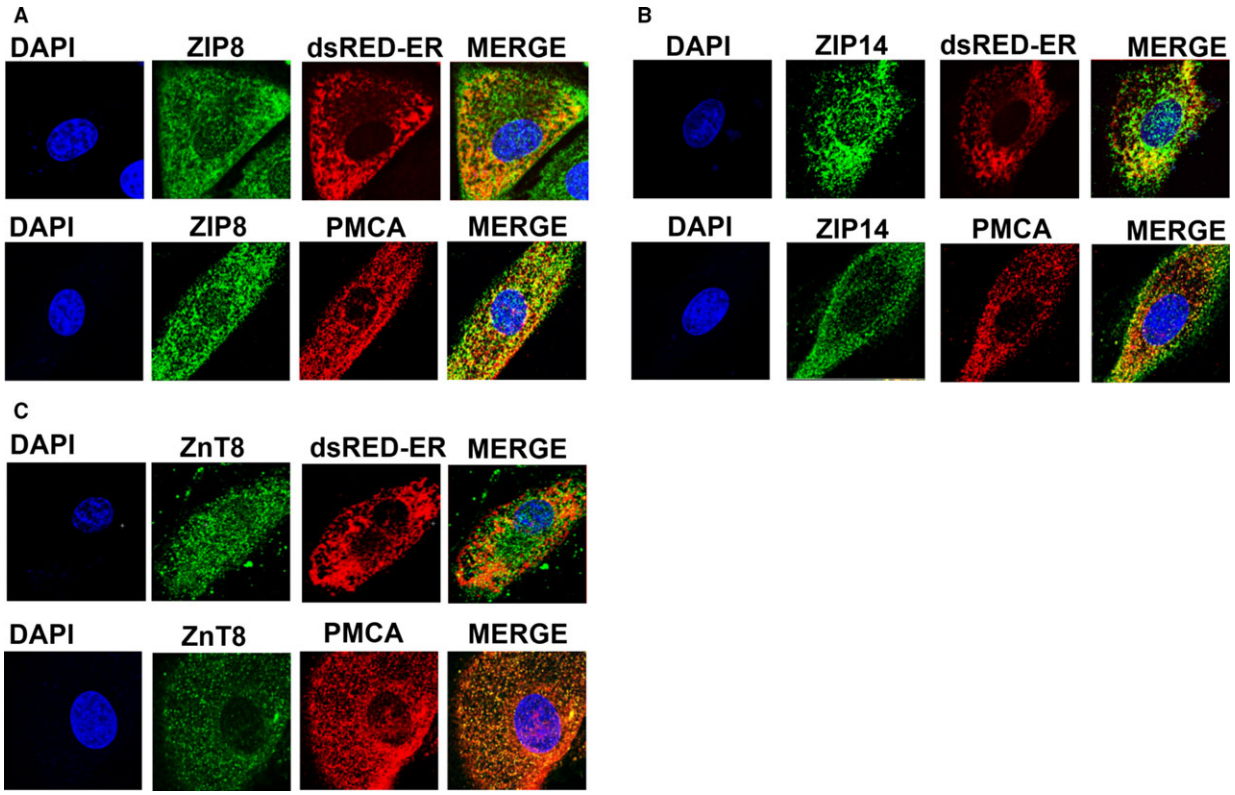


**Fig. 1** Visualization of ZIP8, ZIP14 and ZnT8 localizations in H9c2 cells. Localizations either to the S(E)R or to the sarcolemma/plasma membrane of ZIP8 (**A**), ZIP14 (**B**) and ZnT8 (**C**) were visualized using confocal micrographs in H9c2 cells. To examine the subcellular localizations of these transporters to S(E)R, H9c2 cells were transfected with ER-resident discosoma red fluorescent protein (dsRed-ER) to label ER or incubated with PMCA antibody to label sarcolemma/plasma membrane and with DAPI (blue) as well. Cells were incubated only with secondary antibodies and mounted with mounting medium contains DAPI (blue), and then images were merged.



Journal of Cellular and Molecular Medicine published by John Wiley & Sons Ltd and Foundation for Cellular and Molecular Medicine.

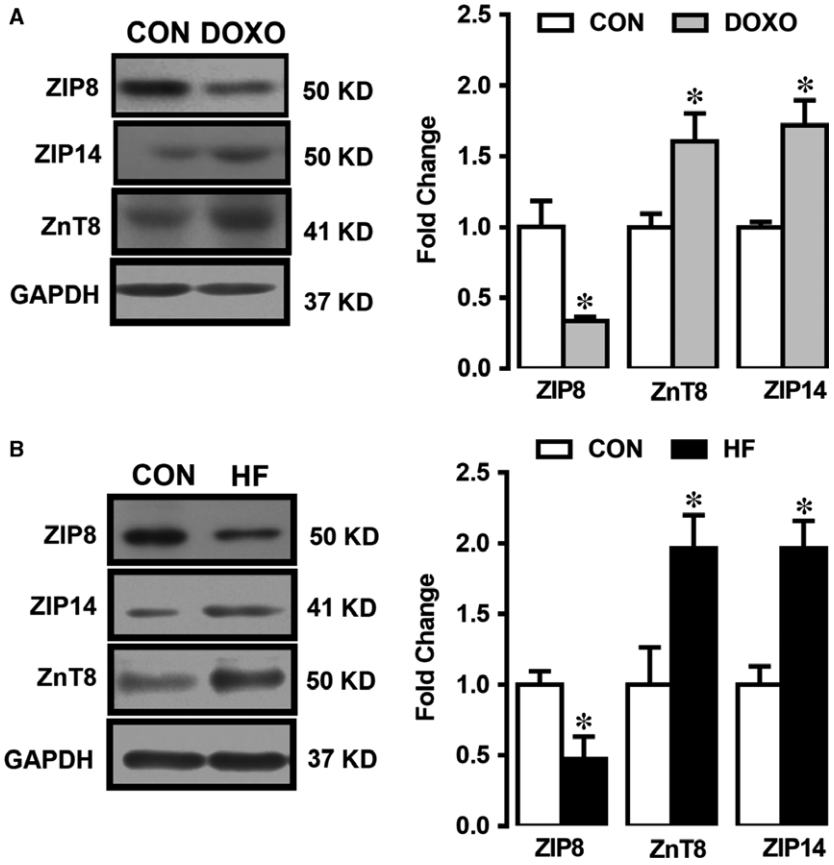


**Fig. 2** Expression levels of ZIP8, ZIP14 and ZnT8 in heart tissue homogenates and doxorubicin-treated H9c2 cells. Representative Western blotting bands for protein expression levels are given left part of figures in (**A**) and (**B**). The densitometry analysis showing the proteins of ZIP8, ZnT8 and ZIP14 is expressed at 50 kD, 41 kD and 50 kD, respectively, in doxorubicin-treated H9c2 cells (DOXO group) with respect to untreated cells (CON group) (**A**) and underwent orthotopic heart transplantation with end-stage heart failure (HF group) with respect to unsuitable for cardiac transplantation patients (CON group) (**B**) GAPDH at 37 kD as reference protein. Bars represent mean (±S.E.M.) for each group. Number of human samples, $n = 3$ for HF group and $n = 2$ for CON group. All measurements with double assays in each sample from each group for each type of measurement. Significance level accepted at $^*P < 0.05$ *versus* CON.

To validate the human heart data related with changes in expression levels of ZIP14, ZIP8 and ZnT8, we also examined the expression levels of these transporters in doxorubicin-treated rat ventricular cells. The observed changes in these transporters were similar to the human data (HF). The expression levels of ZIP14 and ZnT8 were also significantly higher than those of controls while the ZIP8 level was markedly low (Fig. 2B, right). Representative Western blot images are given in the left part of Figure 2B.

## Validation of heart failure in human heart tissue and doxorubicin-treated cells

To correlate diastolic and systolic dysfunction in human HF and deposition of non-sarcomeric alpha ($\alpha$)-actinin (ACTN) in HF and HF-modelled cells, we first measured the ACTN level in underwent orthotopic heart transplantation with end-stage HF with respect to unsuitable for cardiac transplantation patients (CON group). As can be seen from Figure 3A, expression level of ACTN in human tissue (HF group) was significantly high with respect to CON group (left). To confirm further the HF in heart tissues and cell line, we measured the expression level of this biomarker protein, ACTN in doxorubicin-treated H9c2cells. As can be seen in Figure 3A, ACTN level was markedly high in the treated group compared to the untreated group (right).

We also examined the expression level of PUMA (as a pro-apoptotic member of the Bcl-2 family) to further confirmation of heart failure in both human tissues and doxorubicin-treated H9c2 cells. As can be seen in Figure 3B, PUMA protein levels (with respect to GAPDH) were increased markedly in HF group and HF-modelled H9c2 cells comparison with those of their controls (left and right, respectively).

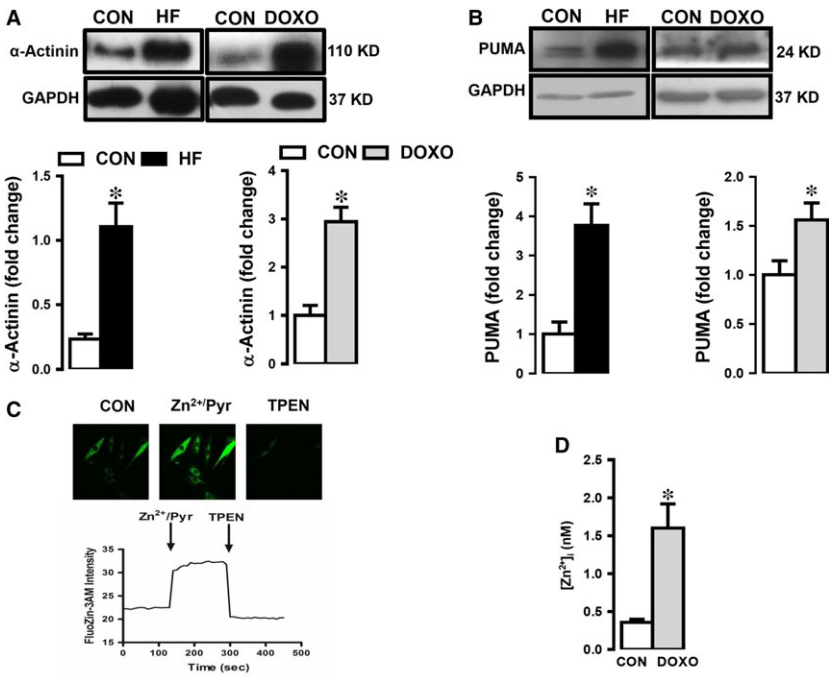


**Fig. 3** Validation of HF in human heart tissue and doxorubicin-treated cells and demonstration of intracellular-free $Zn^{2+}$ increase under HF. (**A**) Expression level of α-actinin, ACTN and PUMA in both human heart tissue with heart failure (HF) (**A**) and doxorubicin (DOXO)-treated H9c2 cells (**B**) with respect to their controls (CON). Representative Western blotting bands for protein expression levels are given upper parts of figures in (**A**) and (**B**). (**C**) Representing of measurement protocol of intracellular-free $Zn^{2+}$, $[Zn^{2+}]_i$ in doxorubicin-treated (failing heart modelled, DOXO group) cells, loaded with $Zn^{2+}$ selective fluorescent dye FluoZin-3. $Zn^{2+}$ ionophore pyrithione, $Zn^{2+}$/Pyr (1-μM) exposure (3 min.) and high-affinity heavy-metal $Zn^{2+}$-chelator, N,N,N',N'-tetrakis(2-pyridylmethyl)ethane-1,2-diamine, TPEN (50 μM). The mean (±S.E.M.) intracellular $Zn^{2+}$level, as FluoZin-3 intensity, respectively. (**D**) Bar graphs representing the $[Zn^{2+}]_i$ levels calculated as nM (see Methods and materials) in the treated cells comparison with the untreated cells (CON group). Bars represent mean (±S.E.M.) for each group. Number of human samples, $n = 3$ for HF group and $n = 2$ for CON group. All measurements with double assays in each sample from each group for each type of measurement. Significance level accepted at $^*P < 0.05$ *versus.* CON.

## $[Zn^{2+}]_i$ increases in doxorubicin-treated cardiomyocytes

To determine $[Zn^{2+}]_i$ in HF-modelled cells, we measured the $[Zn^{2+}]_i$ changes in H9c2 cells loaded with a $Zn^{2+}$ selective and highly sensitive fluorescent dye FluoZin-3. Representative fluorescence intensity changes of FluoZin-3 and experimental protocol are given in Figure 3C. Our data showed that $Zn^{2+}$-ionophore pyrithione, $Zn^{2+}$/Pyr (1 μM) exposure (3 min.) induced significant increase in FluoZin-3 intensity. Further addition of high-affinity heavy-metal $Zn^{2+}$ chelator, N,N,N',N'-tetrakis(2-pyridylmethyl) ethane-1,2-diamine, TPEN (50 μM), FluoZin-3 intensity decreased below its initial value. Of note, in our experiments, the fluorescence loading and $Zn^{2+}$/Pyr-induced changes in $[Zn^{2+}]_i$ changes as well as $[Zn^{2+}]_i$ chelation of $[Zn^{2+}]_i$ in the cells were very sharp and confirmed to be homogenous using confocal images of the loaded cells. The differences between calculated intracellular-free $Zn^{2+}$ levels as nM from normal and doxorubicin-incubated H9c2 cells are given in Figure 3D. As can be seen from the bar graphs, the $[Zn^{2+}]_i$ of the treated cells is about fourfold higher compared to the controls.

## ER stress sensors as molecular chaperones in human HF and doxorubicin-treated H9c2 cells

As GRPs (ER-targeted cytoprotective chaperones, the unfolded-protein response signalling-proteins), as molecular chaperones, are regulated by signal transduction pathways originating in the ER, we first examined the protein expression levels of GRP78, CHOP/Gadd153 and calnexin in the human tissues. Expression levels of GRP78 and CHOP/Gadd153 in human HF group were significantly increased with respect to the controls while no change in calnexin expression level (Figure 4A).

To test whether the inhibition of an endogenous kinase, protein kinase C (PKC), which is generally activated under pathological condition due to different cellular alterations including cellular $Zn^{2+}$ level [22, 23] lead to the suppression of ER stress, we performed another



Journal of Cellular and Molecular Medicine published by John Wiley & Sons Ltd and Foundation for Cellular and Molecular Medicine.

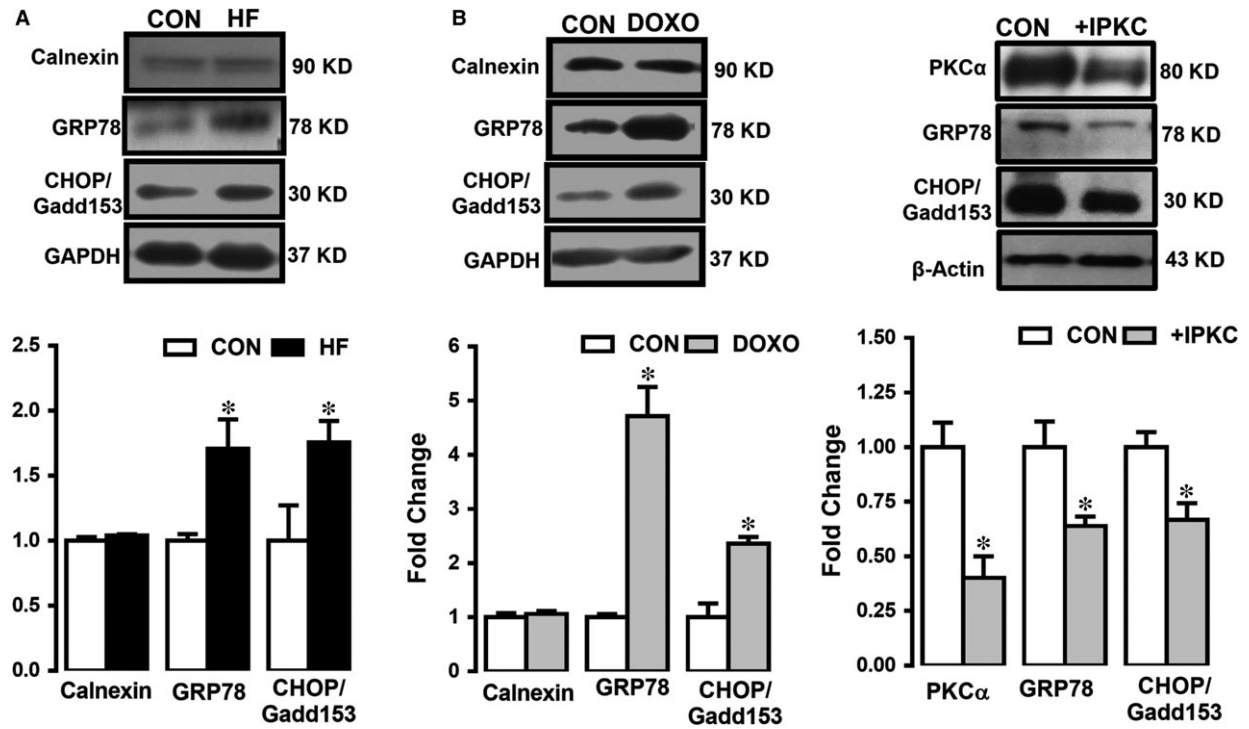


**Fig. 4** Western blot analysis showing the expression levels of ER stress/chaperone proteins in human and doxorubicin-treated H9c2 cells. The densitometry analysis showing the protein levels of GRP78, CHOP/Gadd153 and calnexin at 94 kD, 30 kD and 90 kD, respectively, as well as PKCα activation status detected as protein expression level at 80 kD (with respect to GAPDH at 37 kD) in human heart failure (HF) (**A**) and in doxorubicin (DOXO)-treated H9c2 cells (**B**) with respect to their controls (CON group). Representative Western blotting bands for protein expression levels are given upper parts of figures in (**A**) and (**B**). Bars represent mean (±SEM) for each group. Number of human samples, $n = 3$ for HF and $n = 2$ for CON. Significance level accepted at $^{*}P < 0.05$ *versus* CON and $^{\#}P < 0.05$ *versus* TUDCA group.

group of measurements. As can be seen in Figure 4C, PKC inhibition with an inhibitor (IPKC; incubation of H9c2 cells with 0.1 μM GF109203X hydrochloride for 24 hrs) prevented the induction of ER stress, significantly.

## Verification of increased $[Zn^{2+}]_i$-associated ER stress in doxorubicin-treated H9c2 cells

To verify whether increased $[Zn^{2+}]_i$ underlies the induction of ER stress in HF-modelled H9c2 cells, we first incubated H9c2 cells with $Zn^{2+}$-ionophore pyrithione, $Zn^{2+}$/Pyr (0.1 μM for 24 hrs) and then measured the levels of ER stress chaperones mentioned the previous section. As can be seen from Figure 5A, the expression levels of GRP78, CHOP/Gadd153 and calnexin increased significantly when $[Zn^{2+}]_i$ are increased.

For further confirmation of this experimental approach, in another set of experiments, we measured the expression levels of these markers in the presence of ER stress inhibitor tauroursodeoxycholic acid (TUDCA; 50 μM for 18 hrs) in $Zn^{2+}$/Pyr pre-treated cardiomyocytes. As can be seen from Figure 5A (last columns), the expression of these chaperone proteins was not different from those of controls. These data can suggest a possible association between ER stress induction and increased $[Zn^{2+}]_i$ in human HF.

To understand the involvement of PKCα either under increased $[Zn^{2+}]_i$ or with TUDCA which directly inhibits ER stress, we measured PKCα expression level in these groups. As can be seen in Figure 5A (last column), PKCα expression level was increased significantly under increased $[Zn^{2+}]_i$ with respect to the controls while its level was not changed in ER stress inhibited cells.

## The $[Zn^{2+}]_i$ increase but not a direct ER stress induction underlies the changes in the altered expression levels of $Zn^{2+}$ transporters in HF-modelled doxorubicin-treated H9c2 cells

To verify whether ER stress response activation accounts for cardiomyocyte dysfunction obtained in doxorubicin-incubated H9c2 cells, we examined the expression levels of these chaperones in a direct ER stress activator tunicamycin incubated H9c2 cells (TUN; 10 μM for 18 hrs). As seen in Figure 5B, the expression levels of none of these $Zn^{2+}$ transporters were not changed, significantly. From

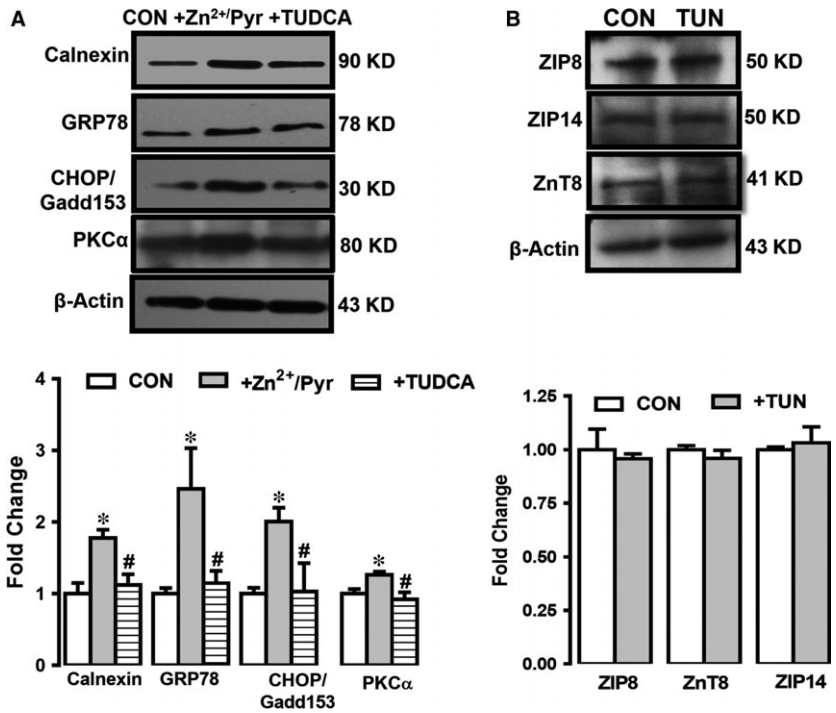


**Fig. 5** Verification of the role of altered expression levels of $Zn^{2+}$ transporters on increased $[Zn^{2+}]_i$-associated ER stress in HF. The ER stress marker proteins such as GRP78, CHOP/Gadd153 and calnexin at 94 kD, 30 kD and 90 kD (with respect to GAPDH at 37 kD) in directly $[Zn^{2+}]_i$ increased H9c2 cells with $Zn^{2+}$ ionophore pyrithione, $Zn^{2+}$/Pyr (0.1 μM for 24 hrs) incubation (without or with an ER stress inhibitor tauroursodeoxycholic acid, TUDCA, 50 μM for 18 hrs) H9c2 cells with respect to their controls (CON) (**A**). The densitometry analysis showing the protein levels of GRP78, CHOP/Gadd153 and calnexin at 94 kD, 30 kD and 90 kD, respectively (with respect to GAPDH at 37 kD). (**B**) The expression levels of ZIP8, ZIP14 and ZnT8 in a direct ER stress activator tunicamycin incubated H9c2 cells (TUN; 10 μM for 18 hrs). All measurements with double assays in each sample from each group for each type of measurement. Significance level accepted at $*P < 0.05$ *versus* CON.

these data, one can provide a hypothesis that ER stress due to any sources cannot directly induce changes in the expression levels of ZIP8, ZnT8 and ZIP14 except increased $[Zn^{2+}]_i$. Therefore, one can further hypothetize that ER stress can be the end process following the changes in these transporters, most probably due to increased $[Zn^{2+}]_i$ in mammalian HF condition.

## The endogenous kinases in failing human heart

To extend our testing on possible association between HF, increased $[Zn^{2+}]_i$ and role of protein kinase-2 (CK2) on triggering $Zn^{2+}$-signalling pathways by phosphorylating $Zn^{2+}$ transporters [29] and contributing to $Zn^{2+}$ homoeostasis, particularly under pathological conditions [20, 30], we measured the expression level of CK2α. As can be seen from Figure 6A, the CK2α level in human HF was not significantly different from that of controls.

As a PKC isoform, PKCα, has been shown to have unique properties among the PKC isotypes such as induction of cardiac hypertrophy [25], regulation of contractility and heart failure susceptibility [26], we aimed to examine this parameter in human HF samples.

The expression level of PKCα was markedly high in human HF group compared to the CON group (Fig. 6C). Furthermore, we also determined the phosphorylation level of PKCα (phospho-PKCα) in the same samples. As can be seen in Figure 6D, the expression level of phospho-PKCα was significantly increased in HF group comparison with the CON group.

## Validation of the role of PKCα-phosphorylation under increased $[Zn^{2+}]_i$ in human HF

To test further the role of PKCα-phosphorylation in $[Zn^{2+}]_i$ increase in mammalian HF, we measured $[Zn^{2+}]_i$ level in both control and doxorubicin-treated cells with and without a total PKC inhibitor (IPKC; 0.1 μM for 24 hrs incubation). As shown in Figure 6E, the increased $[Zn^{2+}]_i$ level in doxorubicin-treated H9c2 cells was significantly decreased while there was also decrease in the untreated cells.



Journal of Cellular and Molecular Medicine published by John Wiley & Sons Ltd and Foundation for Cellular and Molecular Medicine.

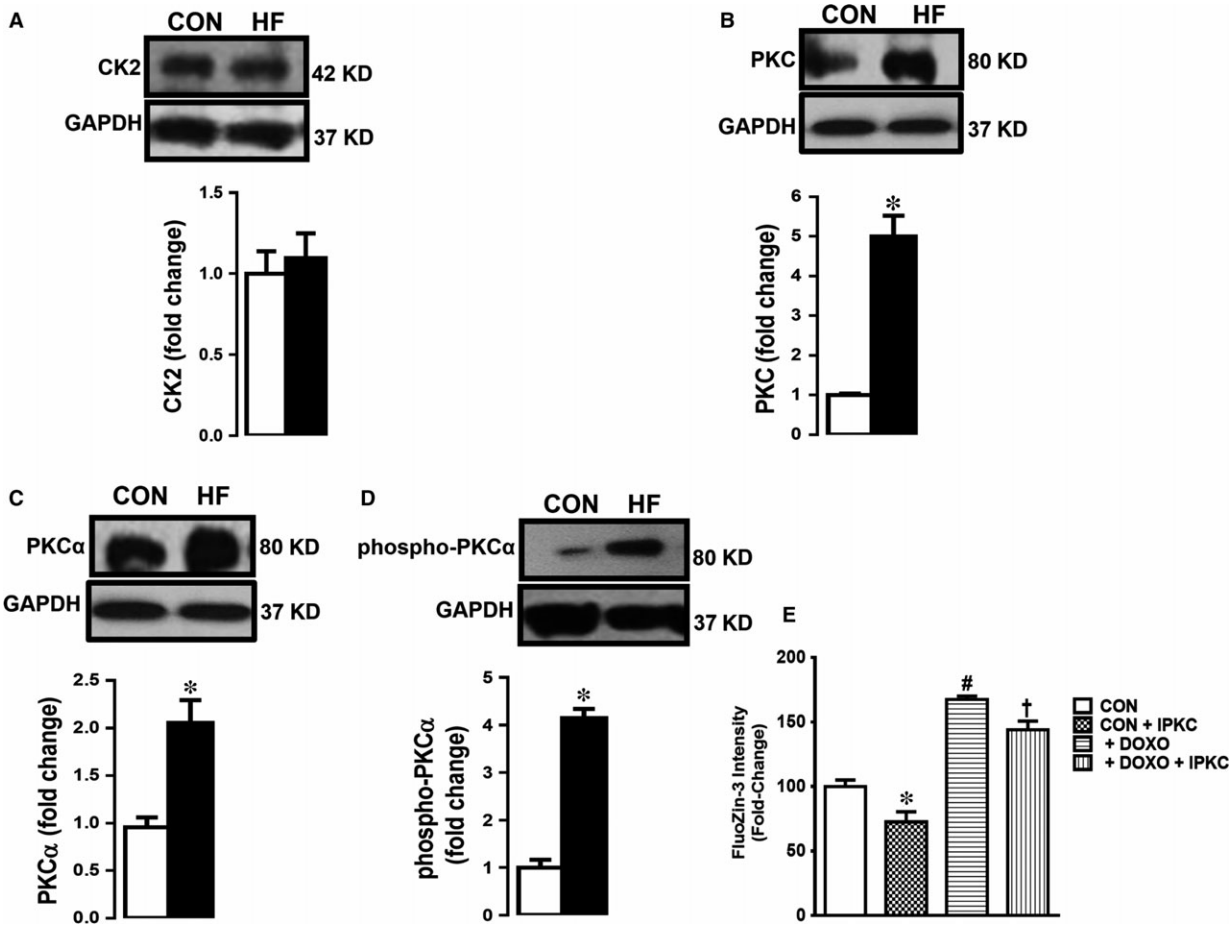


**Fig. 6** Endogenous kinases CK2 and PKC in the human heart tissues. The densitometry analysis of the protein expression levels (Western blotting) given as original bands and mean (±S.E.M.) values for CK2 (α1/α2) in (**A**), total PKC in (**B**), phospho-PKCα (right) and PKCα (left) in (**C**) with respect to GAPDH at 37 kD given for human (HF) and group comparison with the controls. The data were obtained after duplicate assays of each sample from each group for each type of measurement. The number of samples used are the same given in Figure 4 for groups. (**D**) The $[Zn^{2+}]_i$ levels measured in doxorubicin-treated cells with and without a total PKC inhibitor (IPKC GF109203X; 0.1 μM for 24-hrs incubation). Bars represent mean (±S.E.M.). Significance level accepted at $^{*}P < 0.05$ *versus* CON group, $^{\#}P < 0.05$ *versus* CON group and $^{\dagger}P < 0.05$ *versus* DOXO group.

These data are prominent confirmation of association between increased $[Zn^{2+}]_i$ and phosphorylation of PKCα in mammalian HF.

## Discussion

In the present study, we provide evidence to support the crucial role of increased $[Zn^{2+}]_i$ on mammalian heart dysfunction *via* alterations of protein expression levels of $Zn^{2+}$ transporters and induction of ER stress, most probably due to phosphorylation of PKCα. Additionally, our present data further suggest that expression level of some $Zn^{2+}$ transporters together with PKCα activation may play important role in human HF *via* induction of ER stress. Therefore, our observation related with the activation of PKCα under an increased $[Zn^{2+}]_i$ but no change in ER stress markers under PKC inhibition as well as no increase in $[Zn^{2+}]_i$ of the doxorubicin-treated cells under PKC inhibition suggests the possible role of these $Zn^{2+}$–transporters. These information led us to have a conclusion of increase $[Zn^{2+}]_i$ and PKCα-activation (on a way of intersection-pathway associated with them) induced HF, *via* induction of ER stress. Therefore, they have a paramount importance since $[Zn^{2+}]_i$ *via* $Zn^{2+}$ transporters and PKCα may be novel therapeutic approach in prevention/treatment of human HF. Zinc, particularly as $Zn^{2+}$, is essential for human health, and disturbances in its homoeostasis can contribute and/or exacerbate the pathology observed in many chronic conditions including cardiovascular diseases [31–33]. Although $Zn^{2+}$ is required by all cell types, and its toxicity is relatively rare, $[Zn^{2+}]_i$ is tightly controlled under physiological conditions by several ways including specific $Zn^{2+}$ transporters, at most, in redox homoeostasis of the cells [34]. Yet, the overall physiological importance of $[Zn^{2+}]_i$ and $Zn^{2+}$-transporters

at the whole-organism level, particularly their interaction with pathological conditions, remains unclear. We examined possible roles of the $Zn^{2+}$ transporters ZIP8, ZIP14 and ZnT8 in cardiomyocytes under failing condition. For this essential aim, we first examined their protein levels in failing heart preparations. Under any types of heart failure, cardiomyocytes significantly decreased protein level of ZIP8 with markedly increased level of ZIP14 and ZnT8. Additionally, high $[Zn^{2+}]_i$ existence of ER stress together with marked apoptotic status validated the failing heart in our samples. We also, for the first time, presented the subcellular localizations of these transporters in cardiomyocytes. Here, we demonstrated that ZIP8, ZIP14 and ZnT8 localized to both S(E)R and sarcolemma in H9c2 cells, further indicating multiple localization sides for these $Zn^{2+}$ transporter in cardiomyocytes. Taken into consideration a possible crosstalk between increased $[Zn^{2+}]_i$, induction of ER stress and apoptosis in cardiomyocytes, although not assessed directly, it is very logical to hypothesize that any change in any $Zn^{2+}$ transporter under pathological conditions is likely to further exacerbate these changes and contributes to the deleterious consequences of $Zn^{2+}$ redistribution between compartments. Importantly, these transporters are shown to localize into S(E)R membrane and may thus operate as a functional couple catalysing $Zn^{2+}$ release and uptake respectively from the S(E)R while S(E)R is a very good candidate as $Zn^{2+}$ pool [2, 5, 20].

Herein, we have shown a close correlation between $Zn^{2+}$ transporters, $[Zn^{2+}]_i$ and ER stress in failing heart. Our present data demonstrated that ER stress is not induced directly but, our data showed that increased $[Zn^{2+}]_i$ due to alterations in the $Zn^{2+}$ transporters induces ER stress chaperons. ER stress is associated with a range of diseases, including ischaemia/ reperfusion injury and other heart diseases, making ER stress a probable instigator of pathological cell death and dysfunction [35]. The role of ER stress in heart disease has not been extensively studied, but it is well accepted that disturbances in the normal functions of the ER lead to an evolutionarily conserved cell stress response, which is aimed initially at compensating for damage but can eventually trigger cell death if ER dysfunction is severe or prolonged. The principal challenge with any strategy for blocking cell death caused by ER stress lies with the multitude of parallel pathways potentially leading to downstream cell death mechanisms. Thus, blocking only one cell death pathway emanating from the ER may be inadequate to preserve cell survival. Further studies of genes and gene products involved in ER stress-initiated cell death are needed to fully validate targets for drug discovery.

In the present study, we also confirmed the development of HF in human tissue and HF-modelled cardiomyocytes by measuring high level of non-sarcomeric alpha ($\alpha$)-actinin (ACTN). Indeed, correlation between morphological changes, including development of fibrosis, and diastolic and systolic dysfunction together with deposition of ACTN in cardiomyocytes from patients with dilated cardiomyopathy or chronic pressure overload has been shown, previously [36, 37]. Although the precise mechanism of ER stress-induced cardiomyocyte apoptosis remains elusive; it is believed that the mitochondrial apoptotic machinery is recruited through up-regulation of PUMA, a pro-apoptotic member of the Bcl-2 family. Importantly, we and others have shown that any suppression of PUMA activity could prevent both ER stress and ischaemia/reperfusion-induced or diabetes-induced cardiomyocyte loss [38]. In parallel to these data, we also found PUMA levels were increased markedly in all failing heart models compared to the controls suggesting a signalling mechanism related with ER stress-mediated apoptosis.

Although there are several studies related with ZIP8, ZIP14 and ZnT8, there are missing data associated with these transporters and cardiovascular complications. As summary of role of ZIP8 in mammalian cells, Galvez-Peralta *et al.* have shown a critical role of ZIP8-mediated $Zn^{2+}$ transport during in utero and neonatal growth, organ morphogenesis and hematopoiesis while its critical importance was demonstrated for $Zn^{2+}$ cytoprotection in lung epithelia [39]. ZIP14 associated studies pointed out the expression of this transporter in heart tissue besides the other organs in mammalians. Previous studies have shown that ZIP14 is localized at the plasma membrane and in transferrin-containing endosomal compartments [40, 41]. Recent studies demonstrated that the level of ZIP14 protein is increased in the liver of rats fed a high-iron diet and in iron-loaded human hepatoma cells, suggesting that ZIP14 contributes to tissue iron loading under high-iron conditions [41]. A tissue expression array shows that ZIP14 mRNA is ubiquitously expressed with high levels in the liver, pancreas and heart [40].

The ZnT8 is exclusively expressed in pancreatic $\beta$-cells and encodes a protein that transports $Zn^{2+}$ from cytoplasm to insulin secretory vesicles [42]. Additionally, genomewide-associated studies and recent meta-analysis studies demonstrated that a polymorphism

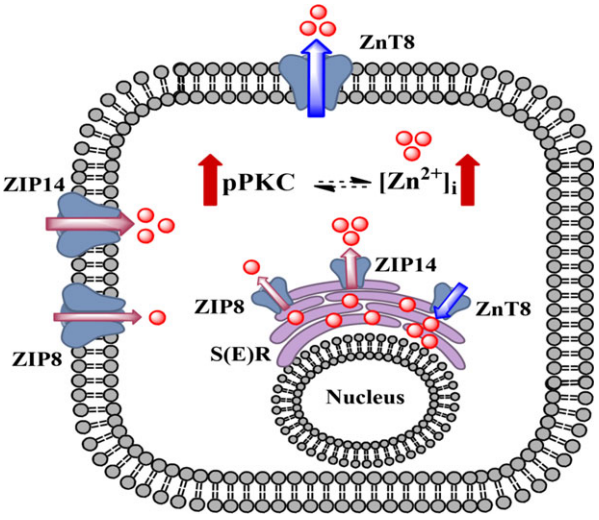


**Fig. 7** A putative summarized presentation of our data on a possible role of $Zn^{2+}$ transporters on an intersection-pathway associated with increased cytosolic free $Zn^{2+}$ and PKC$\alpha$-activation and induction of heart failure *via* development of ER stress. The thickness of the arrows related with the transporters show the alterations in their expression levels. Here, thick red arrows represent increased level of pPKC as phosphorylated PKC$\alpha$ and increased $[Zn^{2+}]_i$, intracellular-free $Zn^{2+}$ concentration in cells under heart failure. The thickness of red arrows related with localization of $Zn^{2+}$ transporters represent increase/decrease expression levels. S(E)R represents sarco(endo)plasmic reticulum.



Journal of Cellular and Molecular Medicine published by John Wiley & Sons Ltd and Foundation for Cellular and Molecular Medicine.

in ZnT8 has closely associated with increased risk of impaired glucose regulation and type 2 diabetes [12, 43, 44]. In studies on multiple $Zn^{2+}$ transporters, such as ZIP8 and ZIP14 or ZIP14 and ZnT10, it has been mentioned that they can be functioning together and thus enhancing their roles in cellular signalling mechanisms [45].

It is well documented that several endogenous substrate proteins of mammalian heart can be phosphorylated with PKC isozymes while they can be activated under pathological conditions including high oxidative stress status *via* thiol oxidation and release of $Zn^{2+}$ from cysteine-rich region of PKC [46, 47]. In here, we have shown that PKC$\alpha$ can be activated under increased $[Zn^{2+}]_i$ in cardiomyocytes while its activation can be prevented by ER stress inhibition. Additionally, we have also shown that if we inhibited PKC$\alpha$, then ER stress can also be inhibited. Therefore, one can suggest that ER stress can be prevented if we have a well-controlled $[Zn^{2+}]_i$ *via* inhibition of PKC$\alpha$ even if under HF. Indeed, studies pointed out the important role of activated PKC$\alpha$ in the heart, as an important mediator of induction of ventricular arrhythmias [48]. It has also been shown that PKC$\alpha$ along with $[Zn^{2+}]_i$ and $Zn^{2+}$ transporters function as effectors of oxidative tissue injury, in part, *via* induction of ER stress [49, 50]. Particularly, PKC$\alpha$ is a specific member of the protein kinase family and is unique in its mode of regulation compared to other kinases within this family. However, it seems CK2 does not underlie any $Zn^{2+}$-related mechanisms in mammalian heart failure, although it has important role in function of cancer cells *via* ZIP7 [40].

A schematic presentation of our present data, given in Figure 7, shows the subcellular distribution of $Zn^{2+}$ transporters, ZIP8, ZIP14 and ZnT8 in ventricular cardiomyocytes. Three of them are localized to both S(E) and sarcolemma and seem to be responsible for the regulation of cellular distribution of free $Zn^{2+}$ under physiological condition. When cardiomyocytes are under pathological condition, leading to heart failure, the expression levels of these three transporters are affected through most probably phosphorylation/activation of PKC$\alpha$, consequently, $[Zn^{2+}]_i$ is increased in cardiomyocytes. In this regard, it has been shown that PKC has ability to regulate many cardiovascular functions *via* targeting many cardiovasotropic growth factors [51], whereas $[Zn^{2+}]_i$ increases the interaction between PKC and actin flaments [23, 52]. Therefore, PKC isoforms could be assessed as possible $Zn^{2+}$ targets and as important regulators of cardiac function under the conditions of ischaemia reperfusion [53]. The increase in $[Zn^{2+}]_i$ under pathological condition further underlies induction of ER stress *via* overexpression of ER stress chaperons in cardiomyocytes which is nicely confirmed with measurement of $[Zn^{2+}]_i$ under a PKC inhibition in doxorubicin-treated cardiomyocytes.

Overall, our present data provide an important insight into the HF in humans, in part, due to the importance of $[Zn^{2+}]_i$, $Zn^{2+}$ transporters and proper excitation–contraction coupling in cardiomyocytes, *via* an association with phosphorylation of PKC$\alpha$. Indeed, $Zn^{2+}$ is an essential cofactor for normal cell function and herein, we have shown that altered expression and function of $Zn^{2+}$ transporters can contribute to the pathogenesis of cardiac disorders through increased ER stress and apoptosis. The expression and regulation of $Zn^{2+}$ transporters in the heart and the toxicity of high $[Zn^{2+}]_i$ to these cells will open new insights into the HF in mammalians as proposing new therapeutic strategy as well as the development of $Zn^{2+}$ containing new markers/sensors to better handle HF in humans.

### Limitations

Further studies are needed to evaluate the role of $[Zn^{2+}]_i$, and $Zn^{2+}$ transporters in advanced HF patients with different aetiologies. Duration of advanced HF and medications also may affect the results.

## Acknowledgements

The authors thank to The Scientific and Technological Research Council of Turkey (TUBITAK) for grant SBAG-113S466 and COST action TD1304.

## Ethical Approval

Patients were eligible to participate in the study and the Local Ethics Committee of Ankara University approved the study protocol (1003201404-142-14).

## Conflict of interest

The authors declare that there is no conflict of interest.

## References

1. **Fauconnier J, Lacampagne A, Rauzier JM, *et al.*** Ca2+-dependent reduction of IK1 in rat ventricular cells: a novel paradigm for arrhythmia in heart failure? *Cardiovasc Res*. 2005; 68: 204–12.
2. **Woodier J, Rainbow RD, Stewart AJ, *et al.*** Intracellular zinc modulates cardiac ryanodine receptor-mediated calcium release. *J Biol Chem*. 2015; 290: 17599–610.
3. **Tuncay E, Okatan EN, Toy A, *et al.*** Enhancement of cellular antioxidant-defence preserves diastolic dysfunction *via* regulation of both diastolic Zn2+ and Ca2+ and prevention of RyR2-leak in hyperglycemic cardiomyocytes. *Oxid Med Cell Longev*. 2014; 2014: 290381.
4. **Turan B, Fliss H, Desilets M.** Oxidants increase intracellular free Zn2+ concentration in rabbit ventricular myocytes. *Am J Physiol*. 1997; 272: H2095–106.
5. **Tuncay E, Bilginoglu A, Sozmen NN, *et al.*** Intracellular free zinc during cardiac excitation-contraction cycle: calcium and redox dependencies. *Cardiovasc Res*. 2011; 89: 634–42.
6. **Kochanczyk T, Drozd A, Krezel A.** Relationship between the architecture of zinc coordination and zinc binding affinity in proteins–insights into zinc regulation. *Metallomics*. 2015; 7: 244–57.
7. **Fukada T, Yamasaki S, Nishida K, *et al.*** Zinc homeostasis and signaling in health and diseases: zinc signaling.

*J Biol Inorg Chem*. 2011; 16: 1123–34.
8. **Maret W.** Zinc and human disease. *Met Ions Life Sci*. 2013; 13: 389–414.
9. **Eide DJ.** Zinc transporters and the cellular trafficking of zinc. *Biochem Biophys Acta*. 2006; 1763: 711–22.
10. **Yang L, Zhao D, Ren J, *et al.*** Endoplasmic reticulum stress and protein quality control in diabetic cardiomyopathy. *Biochem Biophys Acta*. 2015; 1852: 209–18.
11. **Cicek FA, Toy A, Tuncay E, *et al.*** Beta-blocker timolol alleviates hyperglycemia-induced cardiac damage *via* inhibition of endoplasmic reticulum stress. *J Bioenerg Biomembr*. 2014; 46: 377–87.
12. **Bellomo EA, Meur G, Rutter GA.** Glucose regulates free cytosolic Zn(2)(+) concentration, Slc39 (ZiP), and metallothionein gene expression in primary pancreatic islet beta-cells. *J Biol Chem*. 2011; 286: 25778–89.
13. **Meur G, Qian Q, da Silva Xavier G, *et al.*** Nucleo-cytosolic shuttling of FoxO1 directly regulates mouse Ins2 but not Ins1 gene expression in pancreatic beta cells (MIN6). *J Biol Chem*. 2011; 286: 13647–56.
14. **Tuncay E, Okatan EN, Vassort G, *et al.*** ss-blocker timolol prevents arrhythmogenic Ca (2)(+) release and normalizes Ca(2)(+) and Zn(2)(+) dyshomeostasis in hyperglycemic rat heart. *PLoS ONE*. 2013; 8: e71014.
15. **Xu J, Zhou Q, Xu W, *et al.*** Endoplasmic reticulum stress and diabetic cardiomyopathy. *Exp Diabetes Res*. 2012; 2012: 827971.
16. **Zhao N, Gao J, Enns CA, *et al.*** ZRT/IRT-like protein 14 (ZIP14) promotes the cellular assimilation of iron from transferrin. *J Biol Chem*. 2010; 285: 32141–50.
17. **Beharier O, Etzion Y, Katz A, *et al.*** Crosstalk between L-type calcium channels and ZnT-1, a new player in rate-dependent cardiac electrical remodeling. *Cell Calcium*. 2007; 42: 71–82.
18. **Etzion Y, Ganiel A, Beharier O, *et al.*** Correlation between atrial ZnT-1 expression and atrial fibrillation in humans: a pilot study. *J Cardiovasc Electrophysiol*. 2008; 19: 157–64.
19. **Lakshmanan AP, Harima M, Sukumaran V, *et al.*** Modulation of AT-1R/AMPK-MAPK cascade plays crucial role for the pathogenesis of diabetic cardiomyopathy in transgenic type 2 diabetic (Spontaneous Diabetic Torii) rats. *Biochem Pharmacol*. 2012; 83: 653–60.
20. **Tuncay E, Bitirim VC, Durak A, *et al.*** Hyperglycemia-induced changes in ZIP7 and ZnT7 expression cause Zn2+ release from the sarco(endo)plasmic reticulum and mediate er stress in the heart. *Diabetes*. 2017; 66: 1346–58.
21. **Taniguchi M, Fukunaka A, Hagihara M, *et al.*** Essential role of the zinc transporter ZIP9/SLC39A9 in regulating the activations of Akt and Erk in B-cell receptor signaling pathway in DT40 cells. *PLoS ONE*. 2013; 8: e58022.
22. **Nishizuka Y.** Intracellular signaling by hydrolysis of phospholipids and activation of protein kinase C. *Science (New York, NY)*. 1992; 258: 607–14.
23. **Csermely P, Szamel M, Resch K, *et al.*** Zinc can increase the activity of protein kinase C and contributes to its binding to plasma membranes in T lymphocytes. *J Biol Chem*. 1988; 263: 6487–90.
24. **Li W, Wang N, Li M, *et al.*** Protein kinase Calpha inhibits myocardin-induced cardiomyocyte hypertrophy through the promotion of myocardin phosphorylation. *Acta Biochim Biophys Sin*. 2015; 47: 687–95.
25. **Braz JC, Bueno OF, De Windt LJ, *et al.*** PKC alpha regulates the hypertrophic growth of cardiomyocytes through extracellular signal-regulated kinase1/2 (ERK1/2). *J Cell Biol*. 2002; 156: 905–19.
26. **Liu Q, Chen X, Macdonnell SM, *et al.*** Protein kinase C{alpha}, but not PKC{beta} or PKC{gamma}, regulates contractility and heart failure susceptibility: implications for ruboxistaurin as a novel therapeutic approach. *Circ Res*. 2009; 105: 194–200.
27. **Venkatesan B, Prabhu SD, Venkatachalam K, *et al.*** WNT1-inducible signaling pathway protein-1 activates diverse cell survival pathways and blocks doxorubicin-induced cardiomyocyte death. *Cell Signal*. 2010; 22: 809–20.
28. **Sato Y, Fujiwara H, Takatsu Y.** Biochemical markers in heart failure. *J Cardiol*. 2012; 59: 1–7.
29. **Taylor KM, Kille P, Hogstrand C.** Protein kinase CK2 opens the gate for zinc signaling. *Cell Cycle*. 2012; 11: 1863–4.
30. **Grubman A, Lidgerwood GE, Duncan C, *et al.*** Deregulation of subcellular biometal homeostasis through loss of the metal transporter, Zip7, in a childhood neurodegenerative disorder. *Acta Neuropathol Commun*. 2014; 2: 25.
31. **Kimura T, Kambe T.** The functions of metallothionein and ZIP and ZnT transporters: an overview and perspective. *Int J Mol Sci*. 2016; 17: 336.
32. **Davidson HW, Wenzlau JM, O'Brien RM.** Zinc transporter 8 (ZnT8) and beta cell function. *Trends Endocrinol Metab*. 2014; 25: 415–24.
33. **Flannick J, Thorleifsson G, Beer NL, *et al.*** Loss-of-function mutations in SLC30A8 protect against type 2 diabetes. *Nat Genet*. 2014; 46: 357–63.
34. **Oteiza PI.** Zinc and the modulation of redox homeostasis. *Free Radic Biol Med*. 2012; 53: 1748–59.
35. **Oyadomari S, Mori M.** Roles of CHOP/GADD153 in endoplasmic reticulum stress. *Cell Death Differ*. 2004; 11: 381–9.
36. **Heling A, Zimmermann R, Kostin S, *et al.*** Increased expression of cytoskeletal, linkage, and extracellular proteins in failing human myocardium. *Circ Res*. 2000; 86: 846–53.
37. **Hein S, Block T, Zimmermann R, *et al.*** Deposition of nonsarcomeric alpha-actinin in cardiomyocytes from patients with dilated cardiomyopathy or chronic pressure overload. *Exp Clin Cardiol*. 2009; 14: e68–75.
38. **Nickson P, Toth A, Erhardt P.** PUMA is critical for neonatal cardiomyocyte apoptosis induced by endoplasmic reticulum stress. *Cardiovasc Res*. 2007; 73: 48–56.
39. **Galvez-Peralta M, He L, Jorge-Nebert LF, *et al.*** ZIP8 zinc transporter: indispensable role for both multiple-organ organogenesis and hematopoiesis in utero. *PLoS ONE*. 2012; 7: e36055.
40. **Taylor KM, Morgan HE, Johnson A, *et al.*** Structure-function analysis of a novel member of the LIV-1 subfamily of zinc transporters, ZIP14. *FEBS Lett*. 2005; 579: 427–32.
41. **Nam H, Wang CY, Zhang L, *et al.*** ZIP14 and DMT1 in the liver, pancreas, and heart are differentially regulated by iron deficiency and overload: implications for tissue iron uptake in iron-related disorders. *Haematologica*. 2013; 98: 1049–57.
42. **Chimienti F, Devergnas S, Favier A, *et al.*** Identification and cloning of a beta-cell-specific zinc transporter, ZnT-8, localized into insulin secretory granules. *Diabetes*. 2004; 53: 2330–7.
43. **Solomou A, Philippe E, Chabosseau P, *et al.*** Over-expression of Slc30a8/ZnT8 selectively in the mouse alpha cell impairs glucagon release and responses to hypoglycemia. *Nutr Metab (Lond)*. 2016; 13: 46.
44. **Mitchell RK, Hu M, Chabosseau PL, *et al.*** Molecular genetic regulation of Slc30a8/ZnT8 reveals a positive association with glucose tolerance. *Mol Endocrinol*. 2016; 30: 77–91.
45. **Fujishiro H, Yano Y, Takada Y, *et al.*** Roles of ZIP8, ZIP14, and DMT1 in transport of cadmium and manganese in mouse kidney proximal tubule cells. *Metallomics*. 2012; 4: 700–8.
46. **Knapp LT, Klann E.** Superoxide-induced stimulation of protein kinase C *via* thiol

modification and modulation of zinc content. *J Biol Chem*. 2000; 275: 24136–45.

47. **Kooij V, Zhang P, Piersma SR, *et al.*** PKCalpha-specific phosphorylation of the troponin complex in human myocardium: a functional and proteomics analysis. *PLoS ONE*. 2013; 8: e74847.
48. **Mathieu S, El Khoury N, Rivard K, *et al.*** Reduction in Na(+) current by angiotensin II is mediated by PKCalpha in mouse and human-induced pluripotent stem cell-derived cardiomyocytes. *Heart Rhythm*. 2016; 13: 1346–54.
49. **Lyon RC, Zanella F, Omens JH, *et al.*** Mechanotransduction in cardiac hypertrophy and failure. *Circ Res*. 2015; 116: 1462–76.
50. **Xia P, Liu Y, Cheng Z.** Signaling pathways in cardiac myocyte apoptosis. *Biomed Res Int*. 2016; 2016: 9583268.
51. **Feener EP, Northrup JM, Aiello LP, *et al.*** Angiotensin II induces plasminogen activator inhibitor-1 and -2 expression in vascular endothelial and smooth muscle cells. *J Clin Investig*. 1995; 95: 1353–62.
52. **Forbes IJ, Zalewski PD, Giannakis C, *et al.*** Interaction between protein kinase C and regulatory ligand is enhanced by a chelatable pool of cellular zinc. *Biochem Biophys Acta*. 1990; 1053: 113–7.
53. **Prost AL, Bloc A, Hussy N, *et al.*** Zinc is both an intracellular and extracellular regulator of KATP channel function. *J Physiol*. 2004; 559: 157–67.